发光学报
CHINESE JOURNAL OF LUMINESCENCE
中文核心期刊
主管：中国科学院
主办：中国科学院长春光学精密机械与物理研究所
中国物理学会发光分会
主编：申德振

$Sr_2MgSi_2O_7$中本征缺陷和镧系离子的热力学稳定性和转变能级

闻军，汪燕，江贵生，郭海，宁利新

引用本文:
闻军, 汪燕, 江贵生, 等. $Sr_2MgSi_2O_7$中本征缺陷和镧系离子的热力学稳定性和转变能级[J]. 发光学报, 2020, 41(6): 655-663.
WEN Jun, WANG Yan, JIANG Gui-sheng, et al. Thermodynamic Stabilities and Transition Levels of Native Defects and Lanthanide Ions in $Sr_2MgSi_2O_7$[J]. *Chinese Journal of Luminescence*, 2020, 41(6): 655-663.

在线阅读 View online: https://doi.org/10.3788/fgxb20204106.0655

Article ID: 1000-7032(2020)06-0655-09

Thermodynamic Stabilities and Transition Levels of Native Defects and Lanthanide Ions in $Sr_2MgSi_2O_7$

WEN Jun[1,2,3*], WANG Yan[1], JIANG Gui-sheng[1], GUO Hai[4*], NING Li-xin[2,3]

(1. *School of Electronic Engineering and Intelligent Manufacturing, Anqing Normal University, Anqing* 246133, *China*;
2. *The Key Laboratory of Functional Molecular Solids, Ministry of Education, Anhui Normal University, Wuhu* 241000, *China*;
3. *Anhui Key Laboratory of Optoelectric Materials Science and Technology, Anhui Normal University, Wuhu* 241000, *China*;
4. *Department of Physics, Zhejiang Normal University, Jinhua* 321004, *China*)

* *Corresponding Authors, E-mail: jwen@aqnu.edu.cn; ghh@zjnu.cn*

Abstract: The formation energies and thermodynamic/optical transition energy levels of native defects, defect complexes and lanthanide ions in the $Sr_2MgSi_2O_7$ (SMSO) are calculated from hybrid density functional theory (DFT) with the standard PBE0 functional in order to study their contributions to the thermoluminescence (TL) and long-lasting luminescence (LLL) of the material SMSO: Eu^{2+}, Dy^{3+}. The PBE0-calculated formation energies reveal that the defects/complex V_O, Sr_{Mg}, Mg_{Sr} and Sr_{Mg}-Mg_{Sr} are relatively easily generated in the SMSO samples prepared under reducing atmospheres. The thermodynamic and optical transition energy levels of the easily generated defects/complex above and the lanthanide ions in the host are derived from the PBE0-calculated band gap (of 7.18 eV) and formation energies. Based on their comparison with the experimental results of trap depths of the SMSO: Eu^{2+}, Dy^{3+}, the neutral and singly negatively charged V_O and Dy^{3+} ions (at Sr sites) are supposed to act as the electron traps. The aim of this study is to deeply understand the mechanisms of the TL and LLL in the long afterglow material SMSO: Eu^{2+}, Dy^{3+} by using first-principles calculations, which can be adopted as the effective supplement of the experiment.

Key words: native defects; lanthanide ions; thermodynamic transition energy levels; long-lasting luminescence; first-principles

CLC number: O469 **Document code**: A **DOI**: 10.3788/fgxb20204106.0655

$Sr_2MgSi_2O_7$中本征缺陷和镧系离子的热力学稳定性和转变能级

闻 军[1,2,3*], 汪 燕[1], 江贵生[1], 郭 海[4*], 宁利新[2,3]

(1. 安庆师范大学 电子工程与智能制造学院, 安徽 安庆 246133;
2. 安徽师范大学 功能分子固体教育部重点实验室, 安徽 芜湖 241000;
3. 安徽师范大学 光电材料科学与技术安徽省重点实验室, 安徽 芜湖 241000; 4. 浙江师范大学 物理系, 浙江 金华 321004)

摘要: 利用基于标准PBE0泛函的杂化密度泛函理论计算了$Sr_2MgSi_2O_7$中本征缺陷、缺陷复合对及镧系离子的缺陷形成能、热力学转变能级以及光跃迁能级,以研究它们在$Sr_2MgSi_2O_7$: Eu^{2+}, Dy^{3+}的热致发光和长余辉

收稿日期: 2020-04-10; **修订日期**: 2020-04-15
基金项目: 国家自然科学基金(11974315,11974022); 功能分子固体教育部重点实验室开放基金(FMS201908); 安徽省高校优秀青年人才支持计划重点项目(gxyqZD2019046); 安庆师范大学校级教研项目(2019aqnujyzc008)资助
Supported by National Natural Science Foundation of China (11974315, 11974022); Open Project Fund of The Key Laboratory of Functional Molecular Solids, Ministry of Education (FMS201908); Project of Support Program for Excellent Young Talents in Colleges and Universities of Anhui Province (gxyqZD2019046); Teaching Research Project of Anqing Normal University (2019aqnujyzc008)

发光过程中所起的作用。PBE0 计算的形成能结果表明,缺陷 V_O、Sr_{Mg}、Mg_{Sr}和 Sr_{Mg}-Mg_{Sr}较容易在还原气氛下制备的 $Sr_2MgSi_2O_7$ 材料中生成。基于 PBE0 计算的基质带隙(7.18 eV)和缺陷形成能,获得了上述较易形成的缺陷与复合对以及镧系离子的热力学转变能级和光跃迁能级。根据理论计算结果与实验所确定的陷阱深度的直接对比,电中性及带一个负电荷的氧空位与 Dy^{3+} 离子可以作为该材料中的电子陷阱,从而有助于其热致发光和长余辉发光。本研究的目的是利用第一性原理研究方法深入理解 $Sr_2MgSi_2O_7$:Eu^{2+},Dy^{3+} 的热致发光和长余辉发光机理,从而作为实验研究手段的一种有效补充。

关 键 词:本征缺陷;镧系离子;热力学转变能级;长余辉发光;第一性原理

1 Introduction

The phosphor $Sr_2MgSi_2O_7$(SMSO):Eu^{2+},Dy^{3+} is a kind of important long-afterglow material and has many advantages, such as the long afterglow time, high stabilities, non-radiation and so on. Since around 2001[1], researchers have extensively studied this phosphor[1-12], in order to determine the luminescent and trap centers, understand mechanisms of the thermoluminescence(TL) and long-lasting luminescence(LLL), and improve its luminescent properties. It is known that the SMSO:Eu^{2+},Dy^{3+} exhibits a broadband emission, which is ascribed to the electronic transitions from the excited $4f^65d^1$ to the $4f^7$ states of Eu^{2+} ions. Besides, the co-doping of Dy^{3+} ions would enhance the emission intensity, but not affect the position of the emission band.

As for the roles of native defects(anion and cation vacancies) and co-doped lanthanide ions (Dy^{3+}, La^{3+}, Ce^{3+}, Er^{3+} and so on) in the TL and LLL of the material, not only the experimental measurements[1-7] but also the theoretical calculations[8-12] (such as the first-principles and empirical methods) are carried out. It is important to note hereby that the previous first-principles studies on the defective and lanthanide-doped SMSO usually identify the levels related to electron and hole traps according to the Kohn-Sham states from the calculations on band structures or the density of states(DOSs). However, these states should not be confused with the optical transition levels between the different charge states of the same defect/dopant[13], whose locations in the host band gap correspond to trap depths determined from the experimental TL curves of the long afterglow material.

In the present work, hybrid density functional theory (DFT) calculations on formation energies and transition levels of native defects, defect complexes and lanthanide ions in the SMSO are performed in order to theoretically assign the origins of electron traps in the SMSO:Eu^{2+},Dy^{3+}. The calculated formation energies reveal the relatively easily generated defects, whose thermodynamic and optical transition energy levels are further derived. The energy differences between the conduction band minimum (CBM) and the two types of defect levels above respectively give the energies of zero-phonon lines (ZPLs) and electronic transitions for the processes of the electron exchange between native defects (or lanthanide dopants) and the CBM. It is found from this study that the thermodynamic and optical transition energy levels corresponding to the oxygen vacancies with the negative charge states are very close to the CBM. Thus, the corresponding optical transition energies agree well with the experimental trap depths in the SMSO:Eu^{2+},Dy^{3+}. This indicates that the neutral and negatively charged oxygen vacancies are related to the TL and LLL of the SMSO:Eu^{2+}, Dy^{3+}. Besides, the optical transition level of the Dy^{3+} ion at the Sr site is also in a good agreement with the experimental results, confirming that Dy^{3+} ions can be as electron trap centers in the material. It is hoped that the calculations presented in this work are applied to identify the trap centers and analyze the contribution of native defects and lanthanide ions to the TL and LLL of the long afterglow material.

2 Calculation

Geometric optimizations and electronic-structure calculations on the perfect, defective and lanthanide-doped SMSO were performed by using the hybrid DFT with the standard PBE0(Perdew-Burke-

Ernzerhof-0) functional, whose exchange energy is made up of 25% exact Hartree-Fock exchange energy and 75% PBE exchange energy[14-15] (as implanted in the *VASP* software[16-17]). Sr $4s^2 4p_6 5s^2$, Mg $3s^2$, Si $3s^2 3p^2$, O $2s^2 2p^4$ and *Ln* $5s^2 5p^6 4f^{0-14} 5d^{0-1} 6s^2$ (*Ln* = La – Lu) electrons were treated as valence electrons, their interactions with cores were described by the projected augmented wave (PAW) method[18]. Geometry optimizations were performed by using the conjugate gradient technique, and the convergence criteria for total energies and atomic forces were set to be 10^{-5} eV and 10^{-1} eV/nm, respectively. The one Γ point was used for the sampling of the Brillouin zone in the geometric optimizations of the supercells of the SMSO in consideration of the large cost of hybrid DFT calculations with the PBE0 functional. Formation energies (ΔE_f) of the native defects (vacancies and anti-site defects) and complexes in the SMSO are calculated to study their thermodynamic stabilities. The ΔE_f of the defect D in the SMSO is calculated from PBE0-calculated total energies of $1\times1\times2$ supercells, according to the following equation[19-20]:

$$\Delta E_f[D^q] = E_{tot}[D^q] - E_{tot}[\text{perfect}] - \sum_i n_i \mu_i + q(E_F + \varepsilon_{VBM}), \quad (1)$$

where D is in the charge state of q. $E_{tot}[D^q]$ is the total energy of the defective $1\times1\times2$ supercell containing the D^q, and $E_{tot}[\text{perfect}]$ is the total energy of the perfect $1\times1\times2$ supercell which contains 48 atoms. n_i represents the number of the atom i which is doped into ($n_i>0$) or extracted from ($n_i<0$) the perfect $1\times1\times2$ supercell. μ_i represents the chemical potential of the corresponding atoms. E_F is the Fermi level and ε_{VBM} is the position of the valence band maximum (VBM). The chemical potentials of the Sr(μ_{Sr}), Mg(μ_{Mg}), Si(μ_{Si}) and *Ln*(μ_{Ln}) are taken from the PBE0-calculated energies per atom in unit cells of the related bulk materials. The chemical potential of the O atom(μ_O) is derived from the thermal equilibrium conditions for reducing atmospheres (such as H_2/Ar atmospheres[2]):

$$2\mu_{Sr} + \mu_{Mg} + 2\mu_{Si} + 7\mu_O = \mu_{SMSO}, \quad (2)$$

where μ_{SMSO} is the PBE0-calculated total energy of each formula unit of the compound SMSO.

The thermodynamic transition energy level $\varepsilon(q2/q1)$ of the D in the SMSO (as shown in Fig. 1(a)) is defined as the position of the E_F, where the formation energies of the D in the charge states of $q1$ and $q2$ ($q1<q2$) are equal[20]:

$$\varepsilon(q2/q1) = \frac{\Delta E_f[D^{q2}, E_F=0] - \Delta E_f[D^{q1}, E_F=0]}{q1-q2}, \quad (3)$$

where $\Delta E_f[D^{q1}, E_F=0]$ and $\Delta E_f[D^{q2}, E_F=0]$ are the PBE0-calculated ΔE_f of the D^{q1} and D^{q2}, respectively, when the E_F is at the VBM. In the equation (3), the adopted supercells containing the D^{q1} and D^{q2} are in their respective equilibrium configurations. The optical transition energy level $\varepsilon_{opt}(q2/q1)$ of the D in the SMSO is defined similarly, except for that the configuration of the final state is the same as the counterpart of the initial state (as shown in Fig. 1(b)). The processes of the electron exchange between the defect/dopant and the conduction band (CB) are studied according to the locations of the levels $\varepsilon(q2/q1)$ and $\varepsilon_{opt}(q2/q1)$ of the D in the

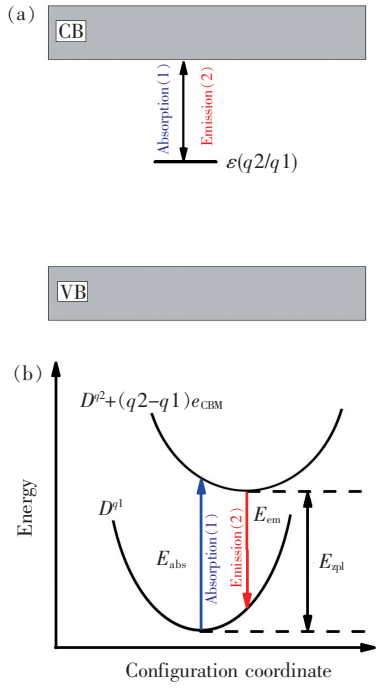

Fig. 1　(a) Schematic representations for the absorption and emission processes associated with the electron exchange between the defect level of the D and the CB. (b) Configuration-coordinate descriptions for the optical transition processes "1" and "2".

band gap of the host. It is seen that the energy of the ZPL(E_{zpl}) for the above process equals to the energy difference between the CBM and the level $\varepsilon(q2/q1)$. Similarly, the energy(E_{abs}) of the absorption process corresponds to the energy difference between the CBM and the level $\varepsilon_{opt}(q2/q1)$.

3 Results and Discussion

The SMSO crystallizes in the tetragonal system and belongs to the $P\bar{4}2_1m$ space group (No. 113), as shown in Fig. 2. The lattice parameters obtained from DFT geometric optimizations with the standard PBE0 hybrid functional are listed in Tab. 1, along with the experimental values[21]. The two sets of values are quite consistent, with relative deviations of less than 0.1%, indicating that the superiority of the PBE0 functional. There are one type of Sr, Mg and Si sites as well as three types of O (labeled as O(1), O(2) and O(3), respectively) sites in the SMSO. The coordination number (CN) of the Sr is eight. The averaged bond length of the Sr—O from the experiment and calculation is 0.267 3 nm and 0.266 8 nm, respectively. Both the Mg and Si are coordinated by four O. The averaged bond length of Mg—O and Si—O from the experiment is 0.189 1 nm and 0.165 5 nm, respectively, with their optimized values of 0.193 8 nm and 0.163 0 nm, respectively. The ionic radii of eight-coordinated Sr^{2+} and four-coordinated Mg^{2+} are 0.126 0 nm and 0.057 0 nm, respectively[22]. The ionic radii of the eight-coordinated Ln^{3+} ions (Ln = La – Lu) are ranging from 0.116 nm to 0.097 7 nm. Besides, the ionic radius of the eight-coordinated Eu^{2+} ion is 0.125 nm. In consideration of the CN and ionic radii of host cations, lanthanide ions are placed at Sr^{2+} sites when their thermodynamic and optical transition energy levels are calculated in order to assign the origins of electron traps in the SMSO.

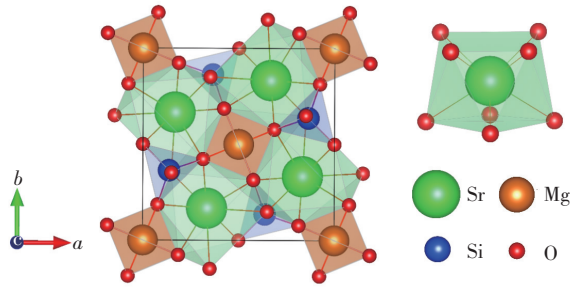

Fig. 2 Schematic diagrams of the unit cell of the SMSO and the local structure around the Sr site

Tab. 1 PBE0-optimized and experimental lattice parameters of the SMSO

Methods	a/nm	b/nm	c/nm	$\alpha=\beta=\gamma$/(°)
Calc.	0.802 0	0.802 0	0.516 1	90.00
Exptl.[21]	0.801 1	0.801 1	0.516 3	90.00

The PBE0-calculated formation energies ΔE_f of native defects and defect complexes in the SMSO are listed in Tab. 2. The ΔE_f of the vacancies at Sr, Mg and Si sites(V_{Sr}, V_{Mg} and V_{Si}) are larger than 10.0 eV, indicating that they are not easily generated in undoped SMSO samples prepared under reducing atmospheres. One may conclude that they are not responsible to the TL and persistent luminescence of SMSO: Eu^{2+}, Dy^{3+} phosphors. Three types of oxygen vacancies ($V_{O(1)}$, $V_{O(2)}$ and $V_{O(3)}$) are easily generated in the host due to their small values of the ΔE_f. Especially, the vacancies prefer to be at O(1) sites with the energy advantages of 31 meV and 231 meV, in comparison with O(2) and O(3) sites, respectively. It should be noted that the ΔE_f of the V_O in the SMSO would increase by 5.533 eV, if the O-rich condition is considered. The ΔE_f of both the anti-site defects Sr_{Mg} and Mg_{Sr} are 1.128 eV and 2.317 eV, respectively, which means that the Sr_{Mg} is much more possible in the host in comparison with the Mg_{Sr}. Moreover, the ΔE_f of defect complexes (V_O-V_{Sr}, V_O-V_{Mg} and Mg_{Sr}-Sr_{Mg}) are also derived to study their thermodynamic stabilities. The two defects in

Tab. 2 PBE0-calculated formation energies ΔE_f of the single defects and defect complexes (with the neutral charge states) in the SMSO

Defects	ΔE_f/eV	Defects	ΔE_f/eV	Defects	ΔE_f/eV
$V_{O(1)}$	0.158	V_{Si}	15.317	$V_{O(2)}$-V_{Sr}	5.525
$V_{O(2)}$	0.189	Sr_{Mg}	1.128	$V_{O(3)}$-V_{Sr}	6.017
$V_{O(3)}$	0.389	Mg_{Sr}	2.317	$V_{O(1)}$-V_{Mg}	4.098
V_{Sr}	11.274	Sr_{Mg}-Mg_{Sr}	2.569	$V_{O(2)}$-V_{Mg}	8.798
V_{Mg}	10.845	$V_{O(1)}$-V_{Sr}	7.596	$V_{O(3)}$-V_{Mg}	4.096

the complex are placed at the nearest-neighbor sites, in consideration of the mutual attraction of their opposite electrical charges of the anion vacancies (V_O) and cation vacancies (V_{Sr} and V_{Mg}). It is found that the ΔE_f of the complexes V_O-V_{Sr} and V_O-V_{Mg} for three types of the V_O are relatively large, further confirming that the V_{Sr} and V_{Mg} are not easily produced in the host. The ΔE_f of the Sr_{Mg}-Mg_{Sr} is 2.569 eV, indicating that this defect complex is possibly generated in the host. This is reasonable since both the single Mg_{Sr} and Sr_{Mg} have the relatively low ΔE_f. It should be noted that the existence of the easily generated defects in phosphors may be confirmed by various experimental measurements, such as the inductive-coupled plasma atomic-emission spectroscopy (ICP-AES)[23] and the electron paramagnetic resonance (EPR)[24].

The PBE0-calculated pattern of the total and orbital DOSs for the perfect 1 × 1 × 2 supercell of the SMSO is illustrated in Fig. 3. It is found that the top of the valence band (VB) is mainly composed of O-2p states, while the bottom of the CB is predominantly constituted by Sr-3d states with the mixture of O-2p states. The band gap of the SMSO calculated from the standard PBE0 hybrid functional is 7.18 eV, much larger than the calculated one (4.69 eV)[9] from the local density approximation (LDA)[25]. According to Hölsä *et al.*[11], the band gap of the SMSO is estimated to be 7.1 eV from the measured synchrotron radiation excitation spectrum of the Eu^{2+}-doped SMSO, which shows a noteworthy increase of the intensity at 175 nm because of the host absorption. The PBE0-calculated value of the band gap is thus in an excellent agreement with the experimentally determined one. It confirms that hybrid DFT calculations with the standard PBE0 functional can efficiently improve the situation of the severe underestimation of the band gaps for the LDA[25] and generalized gradient approximation (GGA)[15] methods. It is noted that an accurate value of the band gap would be crucial for the calculations on the locations of thermodynamic and optical transition energy levels of the defect/dopant in the energy band of the host, further affecting the theoretical assignment of

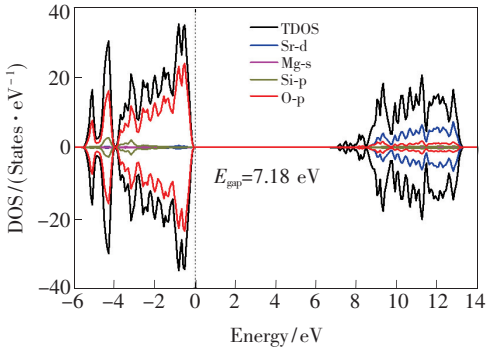

Fig. 3　PBE0-calculated total and orbital-projected DOSs for the 1 × 1 × 2 supercell of the SMSO. The 4 × 4 × 3 *k*-point was adopted for the sampling of Brillouin zone in the calculations of the DOSs.

the origins of the shallow and deep electron traps of long afterglow materials.

The PBE0-calculated defect formation energies ΔE_f as a function of the E_F for the neutral and charged $V_{O(1)}$, $V_{O(2)}$, $V_{O(3)}$, Sr_{Mg}, Mg_{Sr} and Sr_{Mg}-Mg_{Sr} are illustrated in Fig. 4. The defects shown in the figure are relatively easily produced in the SMSO prepared under reducing atmospheres. The location of the E_F in the band gap of the host corresponds to the synthesis conditions of samples[26]. The E_F would be in the upper and lower part of the band gap for reducing and oxidizing atmospheres, respectively. It is in the intermediate region of the band gap when a neutral atmosphere is adopted for the synthesis of samples. In general, the doubly positively charged and neutral V_O in the SMSO is the most stable when the E_F is in the lower and upper part of the band gap, respectively. The doubly negative charge states become the most stable for the V_O, when the E_F is close to the CBM. To take the $V_{O(1)}$ as an example, the 2 + charge state is preferred when the E_F is below 2.657 eV, while the neutral charge state is the most stable when the E_F is in a large region of the band gap (between 2.657 and 6.606 eV above the VBM). Above 6.606 eV, the 2 − charge state is the most stable for the $V_{O(1)}$. The figure also reveals the high similarity between the variation trends of the most stable charge states of the Sr_{Mg}, Mg_{Sr} and their complex Sr_{Mg}-Mg_{Sr} with respect to the E_F. In the most region of the band gap, their neutral charge states are the most stable in energies. This is consistent

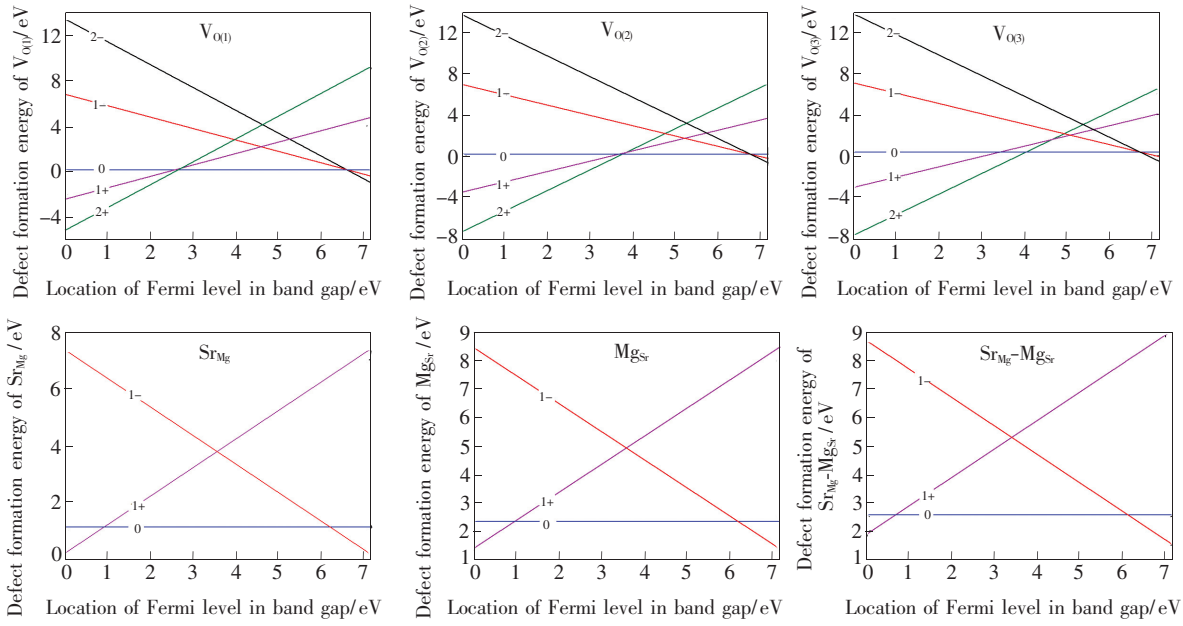

Fig. 4 PBE0-calculated defect formation energies ΔE_f as a function of the Fermi level E_F for the neutral and charged $V_{O(1)}$, $V_{O(2)}$, $V_{O(3)}$, Sr_{Mg}, Mg_{Sr} and Sr_{Mg}-Mg_{Sr} in the SMSO.

with the expectation, considering the same valent states of Sr^{2+} and Mg^{2+} ions.

The intersection between the two lines corresponding to the formation energies ΔE_f of the defect with the charge states $q1$ and $q2$ (as shown in Fig. 4) gives the location of its thermodynamic transition energy level $\varepsilon(q2/q1)$ in the band gap, which is also demonstrated in Fig. 5. The charge state $q2$ is much more stable for the defect/dopant when the E_F is below its level $\varepsilon(q2/q1)$, while the charge state $q1$ is preferred when the E_F is above the level $\varepsilon(q2/q1)$. It is found from the calculated levels $\varepsilon(q2/q1)$ that the V_O with neutral and singly negative charge states in the SMSO may act as electron traps and be responsible to the TL and LLL. The neutral oxygen

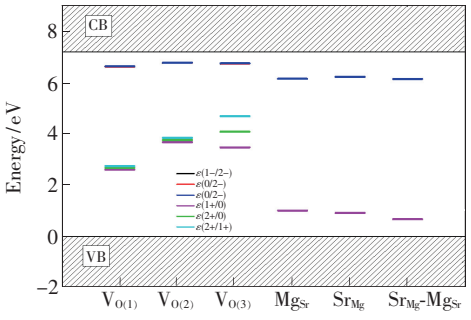

Fig. 5 PBE0-calculated thermodynamic transition energy levels of the $V_{O(1)}$, $V_{O(2)}$, $V_{O(3)}$, Mg_{Sr}, Sr_{Mg} and Sr_{Mg}-Mg_{Sr} in the SMSO.

vacancies V_O are supposed to be stable in the SMSO prepared under reducing atmospheres, as described above. They can capture the electrons released by Eu^{2+} ions when the 4f→5d excitations are carried out, and consequently become negatively charged. After losing an electron (*i. e.*, obtaining a hole "h"), the Eu^{2+} ion turns into the state "$Eu^{2+}+h$". The negative charge states of the V_O are generally metastable except for the situation of the E_F being extremely close to the CBM. The usual thermal activation would promote the electrons of the negatively charged V_O back to the CB. These free electrons can transfer back to the "$Eu^{2+}+h$", generating the 5d→4f emissions. The optical transition energies E_{abs} related to the absorption processes of the electrons from the negatively charged V_O (V_O^{1-} and V_O^{2-}) to the CBM are calculated and listed in Tab. 3. The E_{abs} corresponding to the transformations of the charge states $1- \rightarrow 0$, $2- \rightarrow 0$, and $2- \rightarrow 1-$ for the $V_{O(1)}$, $V_{O(2)}$ and $V_{O(3)}$ are in the range from 0.587 to 0.894 eV, showing a reasonably good agreement with the trap depths determined from the TL curves by Shi *et al.*[5] (0.67 – 0.73 eV) and Hai *et al.*[2] (0.688 – 0.710 eV). Besides, the E_{abs} related to the negatively charged Mg_{Sr}, Sr_{Mg} and Sr_{Mg}-Mg_{Sr} are larger than 1.0 eV, possibly not

contributing to the TL and LLL in the SMSO: Eu^{2+}, Dy^{3+}.

Tab. 3　PBE0-calculated optical transition energies of the native defects and the complex in the SMSO

Defects	$q2/q1$	E_{abs}/eV	E_{zpl}/eV
$V_{O(1)}$	1 −/2 −	0.862	0.577
	0/2 −	0.894	0.571
	0/1 −	0.667	0.565
	1 +/0	5.715	4.587
	2 +/0	6.158	4.516
	2 +/1 +	6.201	4.445
$V_{O(2)}$	1 −/2 −	0.728	0.433
	0/2 −	0.759	0.426
	0/1 −	0.587	0.420
	1 +/0	4.556	3.519
	2 +/0	5.614	3.431
	2 +/1 +	5.912	3.344
$V_{O(3)}$	1 −/2 −	0.751	0.459
	0/2 −	0.784	0.453
	0/1 −	0.598	0.448
	1 +/0	4.871	3.720
	2 +/0	5.746	3.111
	2 +/1 +	5.802	2.503
Mg_{Sr}	0/1 −	1.632	1.051
	1 +/0	6.735	6.175
Sr_{Mg}	0/1 −	1.091	0.973
	1 +/0	6.718	6.269
Sr_{Mg}-Mg_{Sr}	0/1 −	1.242	1.058
	1 +/0	6.741	6.513

The PBE0-calculated locations of the thermodynamic transition energy levels $\varepsilon(1+/0)$ of the dopants Ln (Ln = La − Lu) at Sr sites in the band gap of the SMSO are listed in Tab. 4 and illustrated in Fig. 6. The levels $\varepsilon(1+/0)$ of the Ln_{Sr} correspond to the transformation of trivalent and bivalent states and are conductive to analyze the valence stabilities of lanthanide ions in the host. The hybrid PBE0 calculations indicate that the variation trend of the thermodynamic transition energy levels $\varepsilon(1+/0)$ from La_{Sr} to Eu_{Sr} shows the reasonable similarity with the counterpart from Gd_{Sr} to Yb_{Sr}. Among the two subseries, the Eu and Yb respectively has the lowest level $\varepsilon(1+/0)$, which is in the lower part of the host band gap (2.794 eV and 3.054 eV above the VBM, respectively). This is ascribed to that the 4f orbitals of Eu^{2+} and Yb^{2+} ions are half filled and fully filled, respectively, making their binding energies of 4f electrons much stronger in comparison with the other lanthanide ions. Eu^{2+} rather than Eu^{3+} ions are supposed to be stable in the SMSO prepared under reducing atmospheres, which corresponds to the E_F located in the upper part of the band gap. Eu^{3+} ions may be achieved in the host only if the oxidizing or air atmospheres are adopted[4]. The other trivalent lanthanide ions (such as Dy^{3+} ions[1-3]) are relatively easily obtained in the SMSO under the reducing atmospheres. This may explain the coexistence of bivalent Eu and trivalent Dy ions in the

Tab. 4　PBE0-calculated locations of thermodynamic transition energy levels $\varepsilon(1+/0)$ of the dopants Ln_{Sr} (Ln = La − Lu) in the band gap of the SMSO

Ln	$\varepsilon(1+/0)$/eV	Ln	$\varepsilon(1+/0)$/eV
La	6.390	Tb	6.380
Ce	6.385	Dy	6.399
Pr	6.319	Ho	6.340
Nd	6.056	Er	6.272
Pm	5.794	Tm	5.871
Sm	4.808	Yb	3.054
Eu	2.794	Lu	6.338
Gd	6.352		

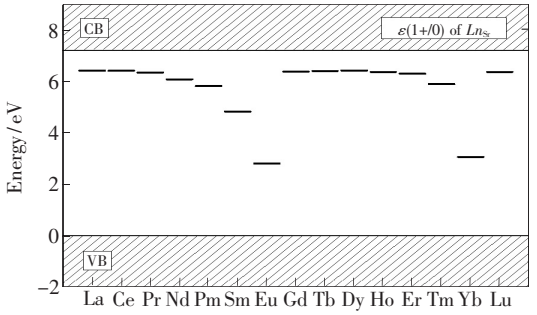

Fig. 6　PBE0-calculated thermodynamics transition energy levels $\varepsilon(1+/0)$ of the dopants Ln_{Sr} (Ln = La − Lu) in the SMSO

material SMSO: Eu, Dy prepared under reducing atmospheres. Moreover, Dy ions (at Sr sites) have the level $\varepsilon(1+/0)$ very close to the CBM, along with their energy separation of 0.781 eV. The E_{abs} for the promotion of the electron from the state "$Dy^{3+}+e$" back to the CBM is calculated to be 0.844 eV, showing a reasonably good agreement with the experimental values (0.67 – 0.73 eV[5] and 0.688 – 0.710 eV[2]) of the trap depths for the SMSO: Eu^{2+}, Dy^{3+}. To sum up, the native defects V_O (with the neutral and 1 – charge states) and co-doped Dy^{3+} ions can serve as electron traps and consequently play an important role in the TL and LLL of the SMSO: Eu^{2+}, Dy^{3+}, according to PBE0-calculated thermodynamic and optical transition energy levels.

4 Conclusion

Thermodynamic stabilities and transition levels of native defects, defect complexes and lanthanide dopants in the SMSO are calculated from the hybrid DFT with the standard PBE0 functional. The band gap of the SMSO host is calculated to be 7.18 eV, agreeing well with the experimental value (of 7.1 eV) determined from the measured synchrotron radiation excitation spectrum of the Eu^{2+}-doped SMSO. The formation energies of cation vacancies (V_{Sr}, V_{Mg} and V_{Si}) are larger than 10.0 eV, indicating that they are not easily generated in the SMSO prepared under reducing atmospheres. Three types of oxygen vacancies ($V_{O(1)}$, $V_{O(2)}$ and $V_{O(3)}$), anti-site defects (Sr_{Mg} and Mg_{Sr}), and the complex Sr_{Mg}-Mg_{Sr} are relatively easily produced under reducing atmospheres. Moreover, the PBE0-calculated thermodynamic/optical transition energy levels and the corresponding energies of the relatively easily generated native defects/complexes and lanthanide dopants demonstrate that the native defect V_O and co-doped Dy^{3+} ions (at Sr sites) can act as electron traps and consequently play an important role in the processes of TL and LLL of the SMSO: Eu^{2+}, Dy^{3+}. It is important to note that the neutral and negatively charged (rather than the positively charged) V_O are involved in the processes of the TL and LLL according to the calculations of this work. Besides, hybrid PBE0 calculations indicate that the variation trend of the thermodynamic transition energy levels $\varepsilon(1+/0)$ from La_{Sr} to Eu_{Sr} shows the reasonable similarity with the counterpart from Gd_{Sr} to Yb_{Sr}. Especially, the location of the level $\varepsilon(1+/0)$ of the Eu is the lowest in the band gap and about 2.794 eV above the VBM.

References:

[1] LIN Y H, TANG Z L, ZHANG Z T, *et al.*. Preparation of a new long afterglow blue-emitting $Sr_2MgSi_2O_7$-based photoluminescent phosphor [J]. *J. Mater. Sci. Lett.*, 2001, 20(16): 1505-1506.

[2] HAI O, REN Q, WU X L, *et al.*. Insights into the element gradient in the grain and luminescence mechanism of the long afterglow material $Sr_2MgSi_2O_7$: Eu^{2+}, Dy^{3+} [J]. *J. Alloys Compds.*, 2019, 779: 892-899.

[3] XIAO L, ZHOU J, LIU G Z, *et al.*. Luminescent properties of R^+ doped $Sr_2MgSi_2O_7$: Eu^{2+}, Dy^{3+} ($R^+ = Li^+, Ag^+$) phosphors [J]. *J. Alloys Compds.*, 2017, 712: 24-29.

[4] LI M H, WANG L L, RAN W G, *et al.*. Tunable Luminescence in $Sr_2MgSi_2O_7$: Tb^{3+}, Dy^{3+} phosphors based on energy transfer [J]. *Materials*, 2017, 10(3): 227-1-11.

[5] SHI C S, FU Y B, LIU B, *et al.*. The roles of Eu^{2+} and Dy^{3+} in the blue long-lasting phosphor $Sr_2MgSi_2O_7$: Eu^{2+}, Dy^{3+} [J]. *J. Lumin.*, 2007, 122-123: 11-13.

[6] SAHU I P, BISEN D P, BRAHME N, *et al.*. Enhanced luminescence performance of $Sr_2MgSi_2O_7$: Eu^{2+} blue long persistence phosphor by co-doping with Ce^{3+} ions [J]. *J. Mater. Sci. Mater. Electron.*, 2016, 27(1): 554-569.

[7] WU H Y, HU Y H, CHEN L, *et al.*. Enhancement on the afterglow properties of $Sr_2MgSi_2O_7$: Eu^{2+} by Er^{3+} cooping [J]. *Mater. Lett.*, 2011, 65(17-18): 2676-2679.

[8] DUAN H, DONG Y Z, HUANG Y, *et al.*. The important role of oxygen vacancies in $Sr_2MgSi_2O_7$ phosphor [J]. *Phys. Lett.* A, 2016, 380(9-10): 1056-1062.

[9] DUAN H, DONG Y Z, HUANG Y, *et al.*. First-principles study of intrinsic vacancy defects in $Sr_2MgSi_2O_7$ phosphorescent

host [J]. *J. Phys.* D: *Appl. Phys.*, 2016,49(2):025304.
[10] HASSINEN J, HÖLSÄ J, LAAMANEN T, *et al.*. Electronic structure of defects in $Sr_2MgSi_2O_7$: Eu^{2+}, La^{3+} persistent luminescence material [J]. *J. Non-Cryst. Solids*, 2010,356(37-40):2015-2019.
[11] HÖLSÄ J, KIRM M, LAAMANEN T, *et al.*. Electronic structure of the $Sr_2MgSi_2O_7$: Eu^{2+} persistent luminescence material [J]. *J. Lumin.*, 2009,129(12):1560-1563.
[12] DORENBOS P. Mechanism of persistent luminescence in $Sr_2MgSi_2O_7$: Eu^{2+}, Dy^{3+} [J]. *Phys. Status Solidi* B, 2005, 242(1):R7-R9.
[13] JANOTTI A, VAN DE WALLE C G. Native point defects in ZnO [J]. *Phys. Rev.* B, 2007,76(16):165202.
[14] ADAMO C, BARONE V. Toward reliable density functional methods without adjustable parameters: the PBE0 model [J]. *J. Chem. Phys.*, 1999,110(13):6158-6170.
[15] PERDEWJ P, BURKE K, ERNZERHOF M. Generalized gradient approximation made simple [J]. *Phys. Rev. Lett.*, 1996,77(18):3865-3868.
[16] KRESSE G, FURTHMÜLLER J. Efficient iterative schemes for *ab initio* total-energy calculations using a plane-wave basis set [J]. *Phys. Rev.* B, 1996,54(16):11169-11186.
[17] KRESSE G, JOUBERT D. From ultrasoft pseudopotentials to the projector augmented-wave method [J]. *Phys. Rev.* B, 1999,59(3):1758-1775.
[18] BLÖCHL P E. Projector augmented-wave method [J]. *Phys. Rev.* B, 1994,50(24):17953-17979.
[19] VAN DE WALLE C G, NEUGEBAUER J. First-principles calculations for defects and impurities: applications to Ⅲ-nitrides [J]. *J. Appl. Phys.*, 2004,95(8):3851-3879.
[20] FREYSOLDT C, GRABOWSKI B, HICKEL T, *et al.*. First-principles calculations for point defects in solids [J]. *Rev. Mod. Phys.*, 2014,86(1):253-305.
[21] OCHI Y. Crystal structure of Sr-akermanite glass-ceramics [J]. *Mater. Res. Bull.*, 2006,41(10):1825-1834.
[22] SHANNON R D. Revised effective ionic radii and systematic studies of interatomic distances in halides and chalcogenides [J]. *Acta Crystallogr. Sect.* A, 1976,32(5):751-767.
[23] KIM T G, LEE H S, LIN C C, *et al.*. Effects of additional Ce^{3+} doping on the luminescence of Li_2SrSiO_4: Eu^{2+} yellow phosphor [J]. *Appl. Phys. Lett.*, 2010,96(6):061904-1-3.
[24] ZHANG J, ZHANG T T, QIU Z X, *et al.*. Fine-tunable self-activated luminescence in apatite-type $(Ba,Sr)_5(PO_4)_3Br$ and the defect process [J]. *Inorg. Chem.*, 2018,57(19):12354-12363.
[25] HOHENBERG P, KOHN W. Inhomogeneous electron gas [J]. *Phys. Rev.*, 1964,136(3B):B864-B871.
[26] DORENBOS P. Valence stability of lanthanide ions in inorganic compounds [J]. *Chem. Mater.*, 2005, 17(25): 6452-6456.

闻军(1987 -),男,安徽桐城人,博士,副教授,2013 年于中国科学技术大学获得博士学位,主要从事稀土发光材料的第一性原理计算的研究。
E-mail: jwen@aqnu.edu.cn

郭海(1980 -),男,江西吉水人,博士,教授,2005 年于中国科学技术大学获得博士学位,主要从事新型稀土光学功能材料的实验研究。
E-mail: ghh@zjnu.cn